Molecular Crystals and Liquid Crystals

Publication details, including instructions for authors and subscription information:
http://www.tandfonline.com/loi/gmcl20

Electroactive Polysilanes: Metastability of Electronic States in Poly[methyl(phenyl)silylene]

S. Nešpůrek [a], G. Wang [a], F. Schauer [b] & F. Kajzar [c]

[a] Institute of Macromolecular Chemistry, Academy of Sciences of the Czech Republic, Prague, Czech Republic

[b] Polymer Centre, Faculty of Technology, T. Bata University in Zlin, Zlin, Czech Republic

[c] Commissariat à l'Energie Atomique, DRT-LIST, DECS/SEMM/LCO, CEA/Saclay, Gif-sun-Yvette, France

Version of record first published: 23 Aug 2006

To cite this article: S. Nešpůrek, G. Wang, F. Schauer & F. Kajzar (2006): Electroactive Polysilanes: Metastability of Electronic States in Poly[methyl(phenyl)silylene], Molecular Crystals and Liquid Crystals, 447:1, 265/[583]-284/[602]

To link to this article: http://dx.doi.org/10.1080/15421400500377305

Mol. Cryst. Liq. Cryst., Vol. 447, pp. 265/[583]–284/[602], 2006

ISSN: 1542-1406 print/1563-5287 online
DOI: 10.1080/15421400500377305

Taylor & Francis
Taylor & Francis Group

Electroactive Polysilanes: Metastability of Electronic States in Poly[methyl(phenyl)silylene]

S. Nešpůrek
G. Wang
Institute of Macromolecular Chemistry, Academy of Sciences of the Czech Republic, Prague, Czech Republic

F. Schauer
Polymer Centre, Faculty of Technology, T. Bata University in Zlin, Zlin, Czech Republic

F. Kajzar
Commissariat à l'Energie Atomique, DRT–LIST, DECS/SEMM/LCO, CEA/Saclay, Gif-sun-Yvette, France

Photoexcitation, photodegradation and metastability of electronic states of poly[methyl(phenyl)silylene] on air and in vacuo are discussed. UV radiation causes the formation of excitons, ion-pairs, free radicals, delocalized positive polarons and scission of Si−Si bonds. Due to the chain deformation during the exciton and polaron formation metastable electronic states 0.45 eV deep originate in vacuo. These states make the conjugation length shorter and can be thermally annealed. On air polysiloxane structures arise.

Keywords: electronic states; metastability; polaron; poly[methyl(phenyl)silylene; polysilane; trapping

INTRODUCTION

A common feature of electronic band structure diagrams for semiconducting polymers is the presence of the energy gap between the

This work was supported by the Grant Agency of the Academy of Sciences of the Czech Republic (Grant No. AV0Z 40500505) and the Ministry of Education, Youth and Sports of the Czech Republic (Grant No. 1P04OC D14.30).

Address correspondence to S. Nešpůrek, Institute of Macromolecular Chemistry, Academy of Sciences of the Czech Republic, Heyrovsky Sq. 2, 162 06 Prague 6, Czech Republic. E-mail: nespurek@imc.cas.cz

highest occupied state and the lowest unoccupied state and of electron levels within them. There is a neutral excitonic level, as the origin of the lowest optical transition, and soliton, polaron and bipolaron ionized levels. An optical excitation leads to a luminescence, phosphorescence or the formation of charge-transfer (CT) states. The CT states can dissociate under the influence of external electric field and free charge carriers can be generated.

Polysilanes (in literature sometimes called polysilylenes, polyorganosilanes, poly(organylsilanediyl)s, organopolysilanes, or catenasilicon polymers) are of considerable research interest because of their electronic, photoelectrical, and non-linear optical properties, and the effect of σ-electron delocalization along the chain [1]. Electron delocalization is perfect if the ratio of the resonance integrals between two sp^3 orbitals located on the same silicon atom and between two sp^3 orbitals located on adjacent silicon atoms are the same. Optical and electrical properties of these polymers have been found to differ significantly from structurally analogous carbon-based σ-bonded systems such as polystyrene and polyethylene, resembling rather fully π-conjugated systems, like polyacetylenes. Physical properties are strongly influenced by the chemical structure of the polymer side groups; thus, different polymers with photoconductive, ionic, thermochromic, piezochromic, photorefractive, electrooptical, non-linear optical, and liquid-crystalline properties can be synthesized [2,3]. Polysilanes, in general are not very stable under UV exposure. It limits their applications in optics and electronics. To bypass this drawback, an extensive search for a stable functionality of tailored polysilanes is under way and the study of their chain stability and degradability is an acute topic of polymer science. Two main effects owing to the UV exposure of polysilane chain can be mentioned: Si–Si bond scission and formation of electronic metastable states (weakened bonds).

The concept of weakened Si–Si bonds (WBs) in σ-conjugated Si linear skeleton, which form localized states for charge carriers was introduced [4] in connection with the origin of visible luminescence in polysilanes. Later studies supported the existence of several luminescence centres with different energy positions and with temperature dependent efficiencies. Alan *et al*. [5] reported, based on the theoretical calculations, that the (σ–σ^*) optical transitions tended to scissor Si−Si bonds; the efficiency of this process strongly depended on interactions with surrounding molecules. However, in some cases WBs could be formed. Takeda *et al*. [6] found by light induced ESR and model calculations two types of photocreated metastable states; one for the low photoexcitation energy ($\sim$3.5 eV) due to the Si skeleton

stretching forces and the other for the higher photoexcitation energy ($\sim$4.8 eV) related to the creation of WBs of inferior quality. The WB concept was also exploited in the model of thermally activated scission of Si–Si bonds; here a distribution of activation energies [7], following the differences in the local atomic configurations and interactions with the surrounding, was used. This model is very close to more general defect-pool one [8] with the distributed creation energies put forward for amorphous silicon a-Si:H and its alloys. The annealing of the metastable states in polysilanes seems to be similar to the observed Staebler-Wronski effect in a-Si:H [9]. However, the one-dimensional Si structure introduces to the metastability problem certain specifications which are discussed in this paper.

LAST RESULTS – SUMMARIZATION

As it was mentioned in the Introduction, the first reference to the polysilane metastability was done by Abkowitz *et al*. [4] in 1987. Latter on, Takeda *et al*. [6] confirmed the existence of metastable states by ESR technique. The long lifetime of the observed light-induced ESR signal at 10 K and the annihilation of the signal by the thermal annealing were consistent with theoretical predictions that some of those excited σ-electrons and σ-holes were trapped with a spatial separation by the difference between their itinerancies sufficiently to suppress their recombination. It led to the charge self-trapping. Thus, especially in real systems at low temperatures the self-trapped charges could be detected (they could be trapped as charge pairs forming dipolar species in the sample). Especially, real polymer chain is a 1 D disordered system rather than a 1 D uniform one, Si skeleton atoms are segmented by some disorderings and distorted bonds, e.g., kinks. These rod-broken points have a potential to become WB centres and can be conserved in the solid state even at room temperature.

Later on an attempt was done to determine the trap depth of WB centres in poly[methyl(phenyl)silylene] (PMPSi) – see Scheme 1, using thermostimulated luminescence (TSL) and post-transient photoconductivity (PTP) measurements. It was found that PMPSi films showed

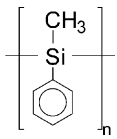

SCHEME 1 Poly[methyl(phenyl)silylene] (PMPSi).

a relatively strong thermoluminescence induced by UV radiation [10,11]. The TSL glow curve consisted of a broad peak with a maximum at $T_m \approx 85$ K. The character of the TSL curve suggested a quasi-continuous trap distribution. The mean activation energy, revealed by the fractional TSL, was determined as $< E_m > = 0.19$ eV, frequency factor as $S \cong 10^{10}$ s^{-1}. Photodegradation of PMPSi films in helium atmosphere at $T \sim 100$ K led to: (i) a slight decrease in the quantum yield of TSL and (ii) to appearance of a notable additional high-temperature shoulder at the main TSL peak in the temperature region of 150–200 K. The drastic changes in TSL glow curves occurred when PMPSi was irradiated with UV light at room temperature. In that case, a new TSL peak with a maximum at about 190 K appeared; its relative intensity became comparable to the intensity of the main TSL peak. The quantum yield of the original TSL simultaneously decreased with the appearance of the new TSL peak. The activation energy and frequency factor in the maximum of the new TSL peak was determined as 0.45 eV and 2×10^{10} s^{-1}, respectively. It should be mentioned that photochemical traps, 0.5 eV deep, were also detected by thermally stimulated current studies [12]. Annealing of these traps, which was also detected by TSL, seems to be interesting from the photochemical metastability of PMPSi. The effect of annealing was possible to fit by the expression of the type $I \sim (1\text{–}\exp(-t/\tau))$, where I is the total TSL intensity (determined as the area under the TSL glow curve), t is the annealing time, and τ is the time constant of the annealing process. The time constants comprised 32.5, 5.6 and 1.6 h for the annealing temperatures 290, 315 and 330 K, respectively. The Arrhenius plot of τ vs. the annealing reciprocal temperature yielded the activation energy of the annealing process equal to ~ 0.65 eV. It should be emphasized that in the case of moderate photodegradation of PMPSi with UV light (total luminescence decreased only to the 50% level) the thermal annealing manifested a complete reversibility and the full recovery of the TSL intensity. It should be pointed out that no additional TSL peak was observed during the UV exposure at liquid helium temperatures. The process of the formation of localized electron states during the sample excitation and degradation was evidently thermally activated.

Provided that the centres 0.45 eV deep, as detected by TSL, represented the charge carrier traps we expected some reversible changes in the shapes of transient photoconductivity signals, especially in post-transient region. The results were obtained by time-of-flight technique [13]. In the transient signal after the laser flash excitation, a current peak followed by plateau and tail was observed. From the intersection of the asymptotes to the plateau and tail the charge

carrier mobility was found as $2.3 \times 10^{-8}\,m^2V^{-1}s^{-1}$ ($F = 3.6 \times 10^7\,Vm^{-1}$, $T = 295\,K$). From the dependences of the mobility on electric field, which was of exp ($\beta F^{1/2}$) form (β is the constant) [14], measured at different temperatures, the zero-field activation energy was determined as E_{a0} ($F \rightarrow 0$) = 0.29 eV. Because we were interested in the elucidation of the formation of localized states during the photodegradation, we also used the post-transit signal analysis for times longer than the transit time. The post-transit signals of partly photodegraded ($\lambda = 340$ nm) PMPSi films were analyzed using the product of current and time; density-of-states (DOS) function $h(E)$ [15] was calculated according to the formula

$$h(E_D) = \frac{2ti(t)}{\rho_{\text{coil}} t_0 \nu} \tag{1}$$

with

$$E_D(t) = kT \ln(\nu t) \tag{2}$$

where $i(t)$ is the photocurrent at time t, ρ_{coil} is the total collected charge, t_0 is the transit time, ν is the attempt-to-escape frequency, E_D is the thermalisation energy, k is the Boltzmann constant and T is the temperature. There were found distributed tail states in a exponential manner with the effective temperature $T_t = 900\,K$. The deep states were found in the energy interval 0.45–0.60 eV; a Gaussian-like distribution was centered around the energy 0.55 eV. These states could be thermally annealed. Surprisingly, the states corresponding to Si–Si dangling bonds in amorphous hydrogenated silicon were generally found at 0.5–0.6 eV [16].

The metastability (reversibility during annealing) was also checked by the measurements of photoluminescence (PL) [11] at low temperatures. The PL spectrum of non-degraded sample consisted of two peaks (cf. Fig. 1) situated at 354 nm and 410 nm. The 366 nm photodegradation at room temperature led to the short-wavelength shift of the exciton band from $\lambda_{\max} \cong 354$ nm to $\lambda_{\max} \cong 344$ nm. It suggested the backbone scission and formation of shorter polymer segments or formation of chain disturbances which limited the effective conjugation length. It should be noted that although the total PL intensity decreased in the course of the photodegradation, some increase in the PL signal at about 520 nm was observed indicating the appearance of an additional emissive band most likely associated with photocreated defects. Thus, visually, the luminescence color shifted from blue (for the non-degraded PMPSi sample) to light-green (for the sample after the photodegradation). It should be noted that the PL band at

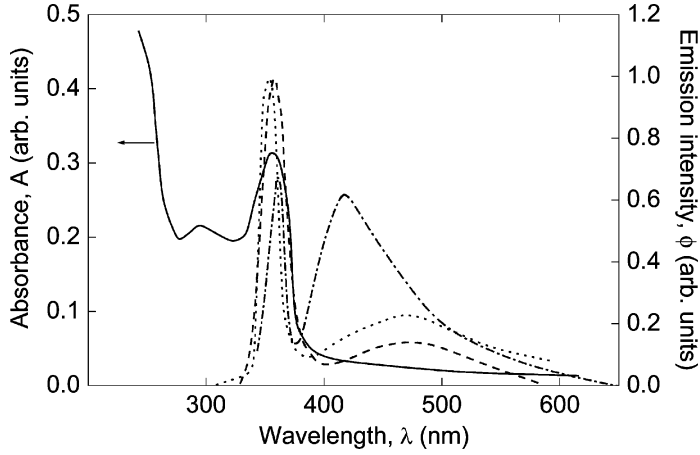

FIGURE 1 Absorption (full line) and photoluminescence (dot line) spectra measured at room temperature. Electroluminescence (dash line) spectrum of ITO/PMPSi/In:Mg diode measured at 77 K. Photoluminescence spectrum measured at 5 K ($\lambda_{exc} = 313$ nm) (dash-and-dot line). Luminescence and electroluminescence curves are normalized to their maxima.

520 nm manifested good reversibility in the case of the moderate photodegradation level; it nearly disappeared after the annealing procedure and the light-green color of the PL at 4.2 K changed back to blue one. This photoluminescence switching effect was well reproducible.

These experiments suggested that during the week photodegradation of PMPSi films the metastable electronic states were formed; they influenced photoelectrical current characteristics, charge carrier trapping and effective conjugation length. To get more information about the metastability in PMPSi, optical absorption, luminescence, electroluminescence and current-voltage characteristics were studied in detail.

EXPERIMENTAL

Materials

Poly[methyl(phenyl)silylene] (PMPSi, see Scheme 1) was prepared by the Wurtz synthesis from the corresponding dichlorosilane. The monomer was reacted with a sodium dispersion in boiling toluene.

Synthesis: 15 g (0.65 g mol) of oxide-free sodium was dispersed in 200 ml of boiling toluene under argon. To increase the yield, 2 ml of diglyme was added to some batches. 50 ml (0.26 mol) of freshly distilled

dichloro(methyl)phenylsilane in 50 ml of toluene was dropped into the dispersion until the colour of the reaction mixture changed to blue, indicating the start of the reaction. The blue colour is explained by defects in the formed NaCl lattice or by sodium colloids. The rest of the monomer solution was added dropwise in the dark during one hour. After the 2 h reaction at 140°C, the reaction was quenched at room temperature by addition of 2 ml of a butyllithium solution (here it was assumed the butyllithium reacted with the rest of chlorine atoms at chain ends and terminated additional reactions and crosslinking). The residual sodium was reacted, under ice cooling, first with 100 ml of ethanol and then with 100 ml of H_2O. The layers were separated, the organic phase was washed three times with 50 ml of H_2O and then dried with anhydrous magnesium sulfate. Crosslinked and insoluble portions were separated by centrifugation with a Beckmann ultracentrifuge J21C at 14000 rpm for 30 min. The polymer was then precipitated by addition of 600 ml of isopropyl alcohol. For purification, it was twice reprecipitated from a THF solution with isopropyl alcohol. The low-molecular-weight portion was separated by 1 h extraction with boiling ether. The polymer was dissolved in THF once again, the solution was centrifuged and the polymer reprecipitated twice from THF with isopropyl alcohol. The polymer was then dried at 13 mbar for 48 h. The yield was 34% (47% when diglyme was used). The residual polymer, obtained in *ca*.17% yield, possessed a unimodal but broad molar mass distribution ($M_w = 4.5 \times 10^4\,\mathrm{g\,mol^{-1}}$, $M_w/M_n = 2.7$, SEC averages relative to polystyrene standards). Molar mass was determined using GPC (Laboratory Instruments, Czech Republic).

Film Fabrication

Thin films (thickness from 70 nm to 1 μm) were prepared from a toluene solution by casting on quartz substrates or conductive ITO glasses. For the measurements of electroluminescence and current-voltage characteristics the top Al or Au electrodes, 40–60 nm thick, were prepared by vacuum evaporation. Before the deposition of films the polymers were three times reprecipitated from a toluene solution with methanol and centrifuged (12000 rpm, 15 min). After the deposition the films were dried at the vacuum of 0.1 Pa at 330 K for at least 4 h. The film thicknesses were determined by surfometric measurements.

Measurements

Photodegradation of samples was performed by UV light from mercury HBO 200 discharge lamp with band filter 340 ± 20 nm. The

degradation process was checked by UV-Vis spectroscopy (Hitachi U300). Photoluminescence (PL) was measured using Hitachi-MPF-4 spectrometer. Electroluminescence was measured on sandwich samples of the type glass/ITO/PMPSi/Al. The emitted light was detected by Hamamatsu C4877 photomultiplier, current-voltage characteristics were measured using Keithley 6517 A electrometer. The samples were kept in a vacuum cryostat (10^{-4} Pa) or under helium or argon during the measurements. In both cases the same experimental results were obtained.

RESULTS

Material Characterization

Polysilanes are photosensitive materials, which degrade quite rapidly during UV irradiation especially in solutions [1]. Their stability can be improved by the attachment of π-conjugated side groups [17]. The quantum yield ϕ_s of the main chain scission at illumination by light 350 nm was found in solid PMPSi as 0.016 fraction of bond per one photon [14] (molecular weight of the photodegraded polymer was determined by gel permeation chromatography). The absorption, photoluminescence (PL) and electroluminescence (EL) spectra of PMPSi film are given in Figure 1. The absorption spectrum consists of two main peaks at about 340 and 276 nm. The long-wavelength band seems to be represented by the cluster of several components [18]. It suggests a disordered phase and a distribution of electronic states above HOMO level and bellow LUMO level (tail states). The Stokes' shift was about 26 nm in solid state. An important difference in the width of the absorption and emission curves should be mentioned; the emission curves are narrower, $\Delta v_{1/2} = 1160\,\mathrm{cm}^{-1}$ vs. $\Delta v_{1/2} = 2430\,\mathrm{cm}^{-1}$ for absorption.

Optical Absorption

As it follows from Figure 2a, the photodegradation led to the decrease of absorption and to the shift of long wavelength maximum to the short wavelength region. It suggested the Si–Si bond scission and/or the limitation of the conjugation length due to the formation of chain disorder, distorted bonds (links) or rod-broken points. When the degradation and spectral measurements were performed in vacuum without any air exposure, a reversible behaviour was observed: the absorbance increased and maximum was shifted to longer wavelengths, as it follows from Figure 2b. It supports the idea of the metastability.

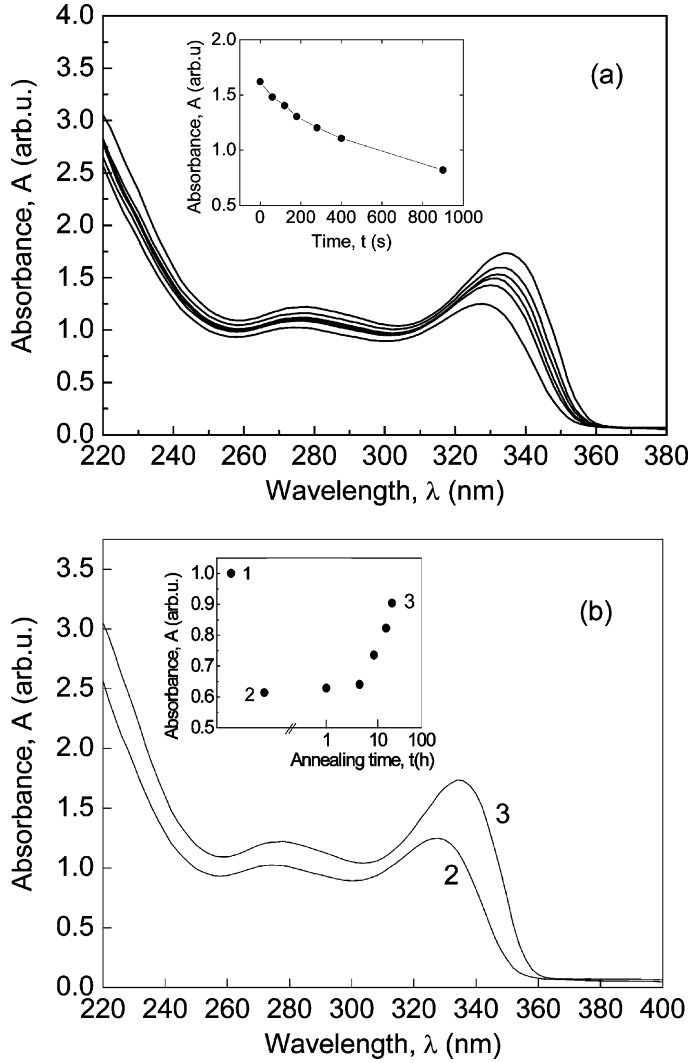

FIGURE 2 (a) Absorption spectrum of PMPSi film (top curve) and spectra after photodegradation with UV light (Hg discharge lamp 200 W, band filter 340 ± 20 nm, room temperature) for the times given in Inset. Decrease in absorbance in the Inset is related to the decrease in the maximum of the long-wavelength band. (b) Reversible change of the absorption spectrum of photodegraded sample (curve 2). Curve 3 represents the spectrum after the annealing of the sample at room temperature for 25 h. The evolution of the absorbance in the maximum of the long-wavelength band is given in the Inset (point 1 – pristine sample, point 2 – photodegraded sample, point 3 – annealed sample). All measurements were made in vacuum at 10^{-3} Pa without any air exposure.

Current–Voltage (j~U) Characteristics

If we assume that the metastable localized states for charge carriers are formed, we must see the trapping effect also on steady-state characteristics of electrical current. In Figure 3 are shown $j \sim U$ characteristics of the samples glass/ITO/PMPSi/Al. Curve 1 represents the dependence for "as prepared" sample, curve 2 the dependence after 30 min illumination of the sample by light from Hg discharge HBO 200 lamp at room temperature. The measurements were performed in vacuum 10^{-3} Pa. The low-voltage parts of the characteristics show the linear and superlinear character followed by strong current increase at about 3 V. The current after the photodegradation was lower by two orders of magnitude. After keeping the sample in dark in vacuum, current increased (curve 3) in agreement with the bleaching of the localized states as observed by TSL experiment. After 15 h the current was obtained nearly on the same level as before the photodegradation.

Electroluminescence

Electroluminescence (EL), which is generated by recombination of electrons and holes injected into the material [19], is very sensitive

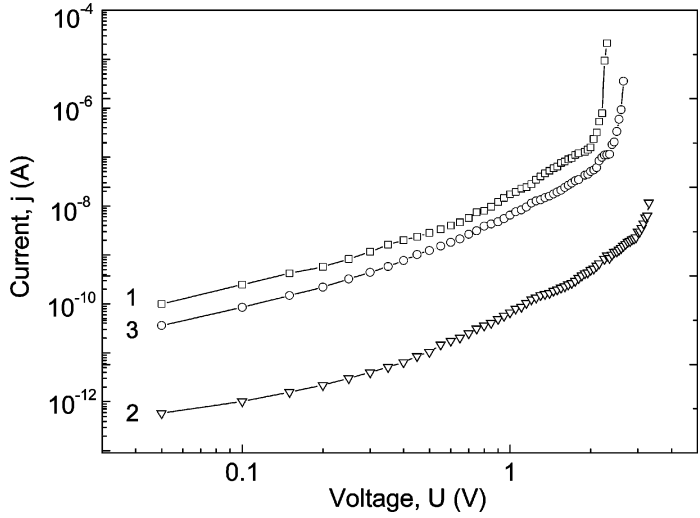

FIGURE 3 Current-voltage characteristics of PMPSi film. Curve 1 – as prepared film; curve 2 – after the photodegradation by light from Hg discharge 200 W lamp for 30 min (band filter $\lambda = 340 \pm 20$ nm); curve 3 – after keeping the sample in vacuum at room temperature for 15 h.

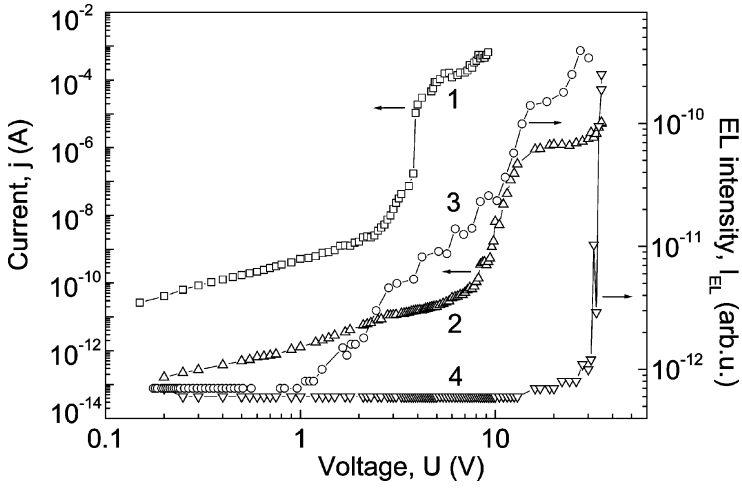

FIGURE 4 Current-voltage characteristics (curves 1 and 2) and the dependences of the electroluminescent intensity on applied voltage (curves 3 and 4). Curves 1 and 3 are for "as prepared" film, curves 2 and 4 for films photodegraded 15 min by Hg 200 W discharge lamp at room temperature in vacuum 10^{-3} Pa.

for the charge carrier trapping. From the spectral distribution of EL (see Fig. 1) it is evident that radiation centres are the same for photo- and electroluminescence [20]. The $j \sim U$ characteristics and dependences light-voltage for a electroluminescent diode ITO/PMPSi/Al (sample thickness was about 280 nm) are shown in Figure 4. The electroluminescence started at about 0.8 V (see curve 3) for "as prepared" sample. After the sample degradation by Hg discharge lamp (15 min, room temperature, vacuum 10^{-3} Pa) the current was lower (cf. curve 2 in Fig. 4), but the shape of $j \sim U$ characteristic remained nearly the same. It was observed a shift of the voltage at which a strong current increase was detected from about 3 to 10 V. It suggests the increase of the charge carrier trap concentration [21] in the sample. The emission threshold of "degraded" sample was shifted from 0.8 to about 20 V. The process was also reversible when measurements were performed in vacuum.

DISCUSSION

Metastability of electronic states in polymers represents a unique process dealt several times with in literature [6,10,11,22] but generally

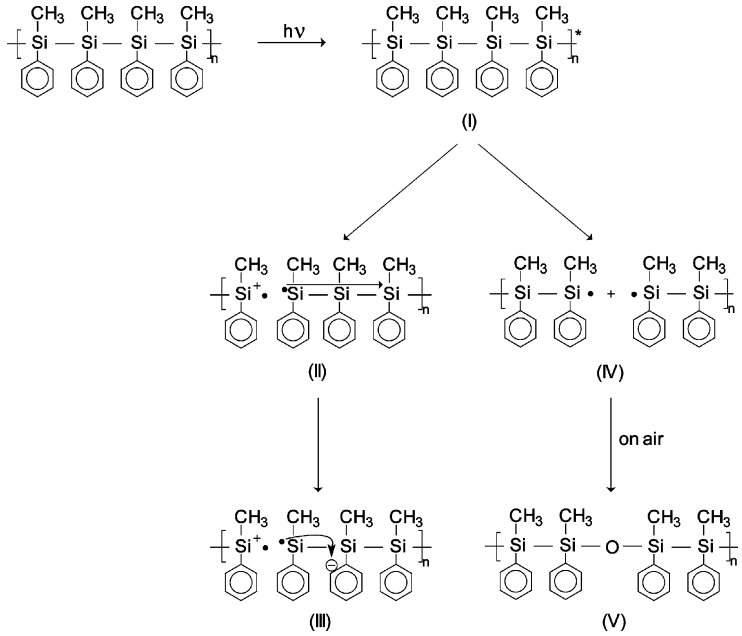

SCHEME 2 Assumed changes of PMPSi chain after excitation.

not fully understood. The illumination of polysilanes leads to several species (see Scheme 2). In the first step an exciton is formed. Back reaction leads to the photoluminecence. An electron from the excited Si–Si bond is transfered from the bonding to antibonding state and due to the σ-conjugation it can move through the polymer chain (see step (II) in Scheme 2). In this way ion-pairs (according to the semiconductor terminology electron-hole pairs) are formed. The antibonding electron can move back and recombine due to electrostatic interaction, or jump to another chain to form inter-chain charge transfer (CT) state, or jump to side group (phenyl in our case) to form intra-chain CT exciton (III). At higher light intensities and long exposure times chain radicals (IV) can be formed. The radicals were checked by flash photolysis [23]. The transient absorption spectra formed during the flash excitation showed two peaks at about 450 and 375 nm. They can be attributed to silylene [24] and localized (i.e. terminal) silyl [25] radicals and/or delocalized cation-radicals [26,27], respectively. The time scale (up to several hundreds of microseconds) of the radical species is sufficiently long for photochemical reactions. The kinetics of the radicals suggest that they can recombine after the photoinduced Si–Si bond scission. However, the photodegradation in air causes the

formation of siloxane species Si–O–Si (see (V) in Scheme 2) as it follows from IR spectrum where additional peaks at 1122 and 1111 cm^{-1} were found [28]. The photodegradation leads to the change in the absorption spectrum as it follows from Figure 2. The long wavelength band located at 340 nm, which arises from delocalized (σ–σ^*) electronic transitions [1], decreases with the level of the photodegradation and its maximum is shifted to the short wavelength region. Because the energy of this transition is conformation dependent and depends strongly on the molar mass and conjugation length of the macromolecule, the excitation energy is effectively deposited almost in the longest all-trans segments; the blue shift of the peak means that Si–Si bond scission exists and conjugation length is shortened. It was demonstrated by the measurement of the decrease of the molar mass during the polymer photodegradation [29]. The peak at shorter wavelengths ($\sim$276 nm for solid PMPSi), which is related to (π–π^*) transitions, decreases with photodegradation too. In vacuum a reversibility in the absorbance during the annealing was detected as it follows from Figure 2b. It means that the defect bonds can be recovered and conjugation length prolonged. This effect was not observed during the photodegradation in air. Photoluminescence experiments led to the similar conclusions [20].

The formation of the polar on-chain ion-pairs was detected by time resolved microwave photoconductivity (TRMP) [30,31]. From the initial rapid decay of the signal the half-life $\tau_{1/2} = (80 \pm 20)$ ns was determined. Using the simple model of diffusion controlled recombination of electrons and holes [32], one can determine from the half-time "on-chain" mobility of holes (cation-radicals) μ_c. The obtained value was $\mu_c = 2 \times 10^{-6}$ $m^2 V^{-1} s^{-1}$. The fast recombination was followed by a slow process; its kinetics could be fitted with a stretched exponential function up to the milliseconds range [31]. This process could be related to the intrachain recombination (Si chain cation-radicals with phenyl anion-radicals) and/or to the interchain electron-hole recombination. The latter value must be close to the zero-field drift microscopic 3D mobility; it was indeed observed (at room temperature μ ($F \rightarrow 0$) $\approx 10^{-9}$ $m^2 V^{-1} s^{-1}$ [14]. It could be pointed out that from the measurements of microwave conductivity the value 2×10^{-9} $m^2 V^{-1} s^{-1}$ [32] was obtained.

Thus, the excitation at 355 nm results in the fast formation of electron-hole pairs in the Si backbone that undergo a fast chain geminate recombination to a significant extent. The remaining portion of ion pairs escape the fast geminate recombination presumably due to the fact that σ-conjugation extents only over a limited number of silicons with the consequence that only electron-hole pairs formed in

the same conformational chain segment can recombine fast. The remainder of electron-hole pairs relaxes to the intramolecular ion-pair $(\sigma, \pi^*)^{CT}$ charge-transfer state – the cation-radical is placed on the main chain, the anion-radical is localized on phenyl ring. This implies a transfer of the electron from the silicon backbone to the pendant phenyl group. The electron transfer from the main chain to phenyl is quite possible because the ground state is predominantly σ_{Si-Si}, i.e., ionization potential $I_p(Si-Si) < I_p(benzene)$ [33].

From the results mentioned above it follows that during the illumination of the polysilane chain the excitons, ion-pairs, charges (polarons after the thermalization), radicals and ion-radicals are formed. It was found from energy transfer experiments [34] that during the excitation a stretching of the Si bond skeleton could exist. A similar situation is expected during the polaron [35] formation (due to the ion-pair dissociation or charge injection from the electrodes). The basic characteristics of the chain morphology changes due to the formation of polaronic charge carriers are the following [35]:

(i) positive polaron – Si–Si bond is stretched from *ca*. 2.350 to 2.380 Å, Si–Si–Si bond angle is smaller in comparison with defect-free chain, cf. 102° vs. 110°;
(ii) negative polaron – Si–Si bond is also stretched, but to lesser extent from *ca*. 2.350 to 2.365 Å, Si–Si–Si bond angle is, on the other hand, larger, cf. 118° vs. 110°.

Thus, during the formation of polarons the chemical bonds are stretched in both cases – it leads to the formation of electronic states in the gap. The negative polaron conformation shows a prolongation of the chain conformation whereas the positive polaron conformation is shrunk because of the changes Si–Si–Si angles. In the first case it leads to the formation of the electronic states outside the gap, in the other case inside the gap [6,34]. The data presented above were taken from the calculation of decamers; with longer chains a more pronounced changes are expected. Theoretically, a stretching length change up to 0.65 Å, a half of the Van der Waals radii for Si, could arise.

The stretching causes a creation of weakened Si bonds (WBs) and corresponding metastable electronic states on the Si skeleton. Electronically, the band-edge states are changed by the formation of WBs as follows [6]: The local Si skeleton-bond stretching weakens pσ bonding character of the highest occupied valence-band (HOVB) state, which is formed of the pσ bonding state between the skeleton Si $3p_x$ atomic orbitals, and destabilizes this state. Therefore, the original HOVB

state energetically shifts upwards and forms a hole-gap states (MHS) localized around the WB site. Conversely, a reduction in the spσ^* antibonding character (the lowest unoccupied conduction-band (LUCB) state is formed of the spσ^* antibonding state between the skeleton Si 2 s and 3p_y atomic orbitals) stabilizes the LUCB state energetically, shifting the original LUCB state downwards; thus electron-gap states (MES) are formed. An appearance of the WB's interrupts the σ-conjugation of the band-edge states (as it follows from absorption and fluorescence experiments, cf. Figure 2 and [20]) and creates the tail states. According to quantum chemical calculations [6] holes are localized at the position of the WB cuter, whereas the tail-state electrons tend to localize at two Si atoms on this WB. The formation of the metastable states in the band gap was found experimentally by ESR technique [6] and by TSL [10,11]). Generally, the electronic structure for PMPSi is given in Figure 5. The electronic excitations in

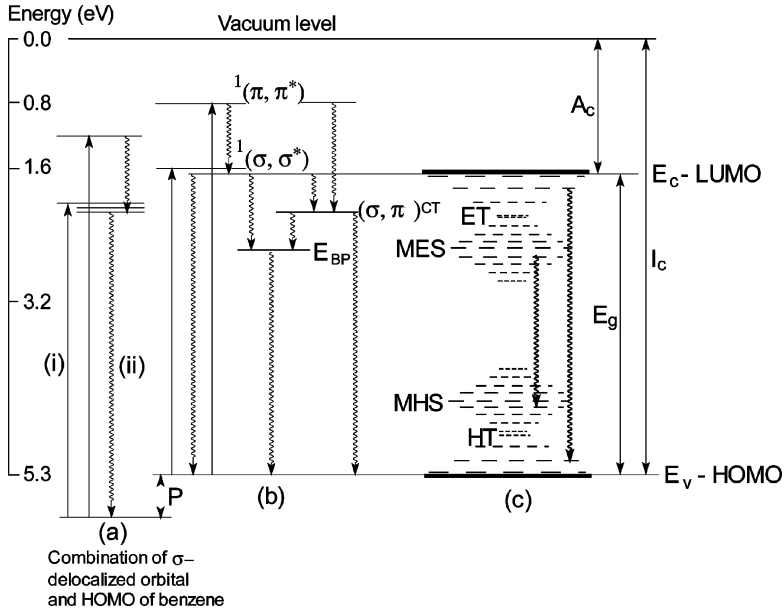

FIGURE 5 Energy diagram of PMPSi: (a) free macromolecule, (b) neutral states in solid state, (c) ionized states in solid state. (i) optical absorption, (ii) luminescence, $(\sigma, \pi^*)^{CT}$ – charge transfer state, A_c – electron affinity, I_c – ionization potential, E_g – energy gap, P – polarization energy, E_{BP} – energy of branching points, ET – electron traps, HT – hole traps, MES – metastable electron states, MHS – metastable hole states.

solution (a) consist mainly from (σ–σ^*) (i) and (π–π^*) (ii) transitions. It holds also in the solid state (b), the HOMO edge being shifted to lower energies by polarization energy P of the polymer by hole. Because of the dispersion of P due to the positional disorder, tail states for holes (HT) and electrons (ET) are formed. It was demonstrated by TSL experiment [10]. The distribution of tail states $h(E)$ could be well approximated by Gaussian distribution, $h(E) \sim \exp(-E^2/2\sigma^2)$ with $\sigma = 0.094$ eV. This value agrees well with the value obtained from the activation energy of the charge carrier mobility [14]. It must be pointed out that a general concept must include a polaron self-trapping – the polaron binding energy is mainly determined by electron-phonon interactions.

Because these metastable gap states for electrons (MES) and holes (MHS) conserve original orbital symmetries of the delocalized band-edge states, optical transitions between them are possible. Thus, these WB's can acts as radiative centres in PMPSi, if the excited electron and hole do not separate spatially. It was observed experimentally using photoluminescence [20]. A discussion of energetics leads to the following conclusion: Absorption maximum at 340 nm from pσ (B_{2g}) to spσ^* (B_{3n}) state reflects the HOVB→LUCB excitation ($=3.5$ eV using a $(h\nu \times \alpha)^2$ vs. hν plot, where hν is the energy of the light quantum and α is the absorption coefficient [18]). The photoluminescence band observed at 520 nm [11] corresponds to the energy 2.4 eV. Thus, the energy difference equals to 1.1 eV. At the first approximation one can assume a symmetry between the electron MES and hole MHS states; thus the energy reduction of the band gap can be divided for electrons and holes; the energy depth can be in this way estimated as 0.55 eV. This value is close to the calculated one from the position of the TSL peak (0.45 eV), from the transient photoconductivity (0.55 eV) and the theoretical estimation [6].

The experiments mentioned above suggest that during the week photodegradation of PMPSi films the metastable electronic states are formed. These states act as trapping centres for charge carriers. The metastability of $j \sim U$ characteristic was demonstrated in Figure 3. The $j \sim U$ characteristic for the pristine sample (curve 1 in Fig. 3) can be analyzed as follows: Two main parts can be distinguished. Low voltage part with linear and superlinear behaviour is followed by strong current jump. The character of the low voltage part of the characteristic is quite complex. One can assume a model of emission-limited current with the participation of traps in the pre-contact region which are formed during the UV sample irradiation. The traps influence the probability of a carrier to cross the barrier formed by the superposition of the image Coulombic and external

potential. The thermoionic emission is given by the equation [36]

$$j \approx A_0 \exp\left(-\frac{E_0}{kT}\right) \exp\left\{-\left[-e\int_0^{x_m} F(x)dx - \frac{e^2}{16\pi\varepsilon\varepsilon_0 x_m}\right] \Big/ kT\right\} \quad (3)$$

with the second exponential term denoting the probability of a carrier to overcome the potential barrier formed by the superposition of the image Coulombic, space-charge and external potentials in the sample. Here, E_0 is the surface energy of the carrier, $F(x)$ is the electric field at distance x from the contact, A_0 is the constant, x_m is the distance of the barrier maximum from the contact, e is the unit charge and $\varepsilon\varepsilon_0$ is the electric permittivity. This equation was solved by Godlewski and Kalinowski [37]; the expression for the current can be written in the form (4)

$$j \approx j_0 \exp(aU^{1/2} - bU^{-1/2}) \quad (4)$$

where

$$a = \frac{e}{kT}\left(\frac{e}{4\pi\varepsilon\varepsilon_0 d}\right)^{1/2} \quad (5)$$

$$b = e\left(\frac{dHv_t\Sigma}{16\pi\varepsilon\varepsilon_0\mu kT}\right)^{1/2} \quad (6)$$

Here, d is the sample thickness, H is the trap concentration, μ is the charge carrier mobility, v_t stands for the thermal velocity of the carriers and Σ for the cross section for the carrier trapping. According to Eq. (4) the current is driven by two processes: the lowering of the Schottky barrier which is proportional to $U^{1/2}$ (thus $j \sim \exp(aU^{1/2})$ and the trap control of the number of carriers arriving at the barrier with sufficient energy to cross it ($j \sim \exp(-bU^{1/2})$). The plot ln j vs. $(aU^{1/2} - bU^{-1/2})$ is given in Figure 6. The low-voltage part of the characteristic gives a good agreement with the proposed model. With increasing trap concentration (MHS states) the current decreases as it follows from the model calculations (see Fig. 7).

The formation of traps during the week photodegradation was tested also by electroluminescence. The experimental characteristics are presented in Figure 4. The curve 1 shows the $j \sim U$ characteristic of the diode ITO/PMPSi/Al. Similarly as in the previous case the low voltage part of the characteristic can be described by emission-limited current. The strong current increase is influenced by charge carrier injection. For higher voltages a transition to $j \sim U^2$ behaviour was found; in this part the current value $j = 1 \times 10^{-4}$ A for $U = 5.1$ V agrees well with the prediction of the space-charge-limited current

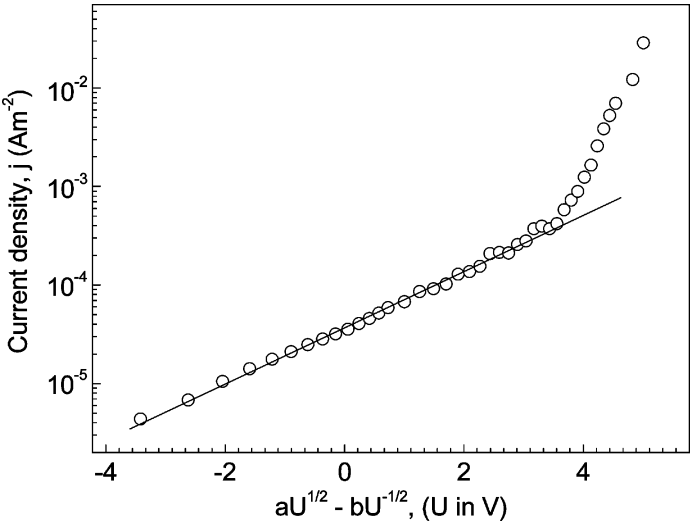

FIGURE 6 Reploted current-voltage ($j \sim U$) characteristic of PMPSi film (curve 1 in Fig. 3) in the coordinates log j vs. ($aU^{1/2} - bU^{-1/2}$) (see text for details).

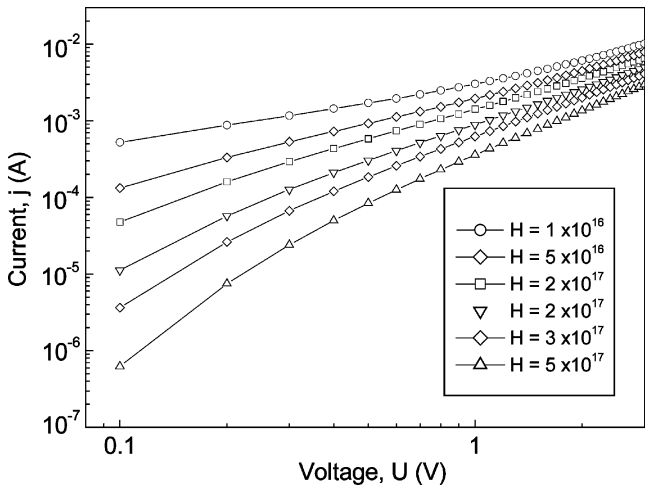

FIGURE 7 Theoretical current-voltage characteristics for thermoionic emission with charge trapping. Number of traps per cm^3 in the barrier H is mentioned in the figure; $j_0 = 10^{-3}\ A\,m^{-2}$.

(SCLC, if the charge carrier mobility is taken as 2×10^{-8} $m^2 V^{-1}$ s^{-1} [14]). Because SCLC theory could be also applied to the high-voltage part of the characteristic, the strong current increase give to us an information on trap-filled-limit voltage U_{TFL} and trap filling. The $j \sim U$ characteristic of photodegraded sample is presented in Figure 4 as curve 2. For low voltages the current is lower which agrees with above mentioned discussion. The voltage at which the strong current increase was observed (U_{TFL}) was shifted to higher voltages; it documents the higher charge carrier trap concentration. The trap-filled-limit voltage U_{TFL} [21] at which the strong current increase is observed is given by the expression

$$U_{TFL} \approx \frac{eHd^2}{\varepsilon\varepsilon_0}. \tag{7}$$

The increase of U_{TFL} from 20 to 30 V (see Fig. 3) represents the 50% increase in the trap concentration. The decrease of the current in the $j \sim U^2$ region and its shift to higher voltages (see Fig. 4) suggests that charge carrier mobility decreases. The rough estimation gives the mobility value about three orders of magnitude lower.

The electroluminescence is related to the charge injection, recombination of electrons and holes and a formation of excitons. Thus, the light emission is expected in the region of the strong current increase. It is roughly fulfilled (cf. curve 3 in Fig. 4). After the week degradation (cf. curve 4 in Fig. 4) the light emission was negligible up to 30 V. It could be mentioned that also electroluminescence intensity followed the sample metastability.

CONCLUSION

The irradiation of PMPSi solid samples in the range of the lowest photoexcitation ($\sim$3.5 eV) leads to the formation of several species, as excitons, polarons, ion-pairs, chain radicals and delocalized cation-radicals. Excitons, polarons and ion-pairs cause the Si–Si bond stretching which results in formation of additional local states in the gap. They are metastable, if sample is irradiated in inert atmosphere or in vacuum, and can be anihilated by heating. These states were detected by several techniques: photoluminescence, thermostimulated luminescence and transient photocurrents. In this paper the metastability was documented using the methods of optical absorption, electrical conductivity and electroluminescence. The metastability could be in future utilized for the preparation of photo/electro responsive polymers without functional side groups and for the fabrication of memory elements.

REFERENCES

[1] Miller, R. D. & Michl, J. (1989). *Chem. Rev.*, *89*, 1359.
[2] Chayase, S. (1994). *Chemtech*, *24*, 19.
[3] Kmínek, I., Nešpůrek, S., Brynda, E., Pfleger, J., Cimrová, V., & Schnabel, W. (1993). *Collect. Czech. Chem. Commun.*, *58*, 2337.
[4] Abkowitz, M., Knier, F. E., Yuh, H.-J., Weagley, R. J., & Stolka, M. (1987). *Solid State Commun.*, *62*, 547.
[5] Allan, G., Delerue, C., & Lannoo, M. (1931). *Phys. Rev. B*, *48*, 7951.
[6] Takeda, K., Shiraishi, K., Fujiki, M., Kondo, M., & Morigaki, K. (1994). *Phys. Rev. B*, *50*, 5171.
[7] Nakayama, Y., Kurando, T., Hayashi, H., Oka, K., & Dohmaru, T. (1996). *J. Non-Cryst. Solids.*, *198–200*, 657.
[8] Davis, E. A. J. (1996). *Non-Cryst. Solids*, *198–200*, 1.
[9] Staebler, D. L. & Wronski, C. R. (1997). *Appl. Phys. Lett.*, *31*, 292.
[10] Kadashchuk, A., Ostapenko, N., Zaika, V., & Nešpůrek, S. (1998). *Chem. Phys.*, *234*, 285.
[11] Kadashchuk, A., Nešpůrek, S., Ostapenko, N., Skryshevskii, Yo., & Zaika, V. (2001). *Mol. Cryst. Liq. Cryst.*, *355*, 413.
[12] Sanda, P. N., Samuel, L., & Miller, R. D. *Proceedings, 3rd Int. SAMPE Electronic Conf.*, June 1989, p. 711.
[13] Schauer, F., Handlíř, R., & Nešpůrek, S. (1997). *Adv. Mater. Opt. Electron*, *7*, 61.
[14] Nešpůrek, S. & Eckhardt, A. (2001). *Polym. Adv. Technol.*, *12*, 427.
[15] Noolandi, J. (1977). *Phys. Rev. B*, *16*, 4466.
[16] Street, R. H. (1991). *Hydrogenated Amorphous Silicon. Series: Cambridge Solid State Science Series*, Cambridge University Press: Cambridge, UK.
[17] Kmínek, I., Brynda, E., & Schnabel, W. (1991). *Eur. Polym. J.*, *27*, 1073.
[18] Navrátil, K., Šik, J., Humlíček, J., & Nešpůrek, S. (1999). *Optical Materials*, *12*, 105.
[19] Rothberg, L. J. & Lovinger, A. J. (1996). *J. Mater. Res.*, *11*, 3174.
[20] Nešpůrek, S., Kadashchuk, A., Skryshevski, Yu., Fujii, A., & Yoshino, K. (2002). *J. Luminescence*, *99*, 131.
[21] Nešpůrek, S. & Sworakowski, J. (1990). *Radiat. Phys. Chem.*, *36*, 3.
[22] Naito, H., Zhang, S. C., Okuda, M., & Dohmaru, T. (1994). *J. Appl. Phys.*, *76*, 3612.
[23] Nešpůrek, S. (1999). *Czech. J. Phys.*, *49*, 859.
[24] Karatsu, T., Miller, R. D., Šooriyakumaran, R., & Michl, J. (1989). *J. Am. Chem. Soc.*, *111*, 1140.
[25] Irie, S. & Irie, M. (1992). *Macromolecules*, *25*, 1766.
[26] Eckhardt, A. & Schnabel, W. (1996). *J. Inorg. Organomet. Polym.*, *6*, 95.
[27] Eckhardt, A., Nešpůrek, S., & Schnabel, W. (1994). *Ber. Bunsen-Ges. Phys. Chem.*, *98*, 1325.
[28] Meszároš, O., Schmidt, P., Pospíšil, J., & Nešpůrek, S. (2004). *J. Polym. Sci., Ser. A, Polym. Chem.*, *42*, 714.
[29] Nešpůrek, S., Schauer, F., & Kadashchuk, A. (2001). *Chem. Monthly*, *132*, 159.
[30] Nešpůrek, S., Herden, V., Kunst, M., & Schnabel, W. (2000). *Synt. Met.*, *109*, 309.
[31] Nešpůrek, S., Toman, P., & Sworakowski, J. (2003). *Thin Solid Films*, *438–439*, 268.
[32] Frey, H., Möller, M., de Haas, M. P., Zenden, N. J. P., Schouten, P. G., van der Laan, G. P., & Warman, J. M. (1993). *Macromolecules*, *26*, 89.
[33] Pitt, C. G., Carey, R. N., & Toren, E. C., Jr. (1972). *J. Am. Chem. Soc.*, *94*, 3806.
[34] Mintmire, J. W. (1989). *Phys. Rev. B*, *39*, 13350.
[35] Toman, P., Nešpůrek, S., Jang, J. W., & Lee, C. E. (2002). *Current Appl. Phys.*, *2*, 327.
[36] Frank, R. I. & Simmons, J. G. (1967). *J. Appl. Phys.*, *38*, 832.
[37] Godlewski, J. & Kalinowski, J. (1979). *Phys. Stat. Sol. (a)*, *56*, 293.